A Mossbauer study on solid krypton precipitates in aluminium

1993 J. Phys.: Condens. Matter 5 3541

(http://iopscience.iop.org/0953-8984/5/22/006)

J. Phys.: Condens. Matter 5 (1993) 3541–3554. Printed in the UK

A Mössbauer study on solid krypton precipitates in aluminium

M J W Greuter and L Niesen

Nuclear Solid State Physics, Groningen University, Nijenborgh 4, 9747 AG Groningen, The Netherlands

Received 27 January 1993, in final form 17 March 1993

Abstract. Mössbauer spectroscopy on the 9.40 keV transition ^{83}Kr is used to obtain information about solid Kr precipitates in Al. Three different ^{83}RbI sources differing in water content were used, which, when measured against a solid Kr absorber, show a quadrupole component in addition to a dominating single line. An analytical deconvolution technique is presented which takes care of the source characteristics. The spectra of Kr bubbles in Al obtained by high-dose implantation show two components: a single line from Kr atoms inside the bubble and a quadrupole split component from Kr at the Kr–Al interface. Spectra were taken as a function of temperature. The total absorption area could be fitted very well assuming a simple Debye model, yielding a Debye temperature of $\Theta_D^T = 101(2)$ K. A decomposition of the total area in the areas of quadrupole and single-line components yields Debye temperatures of $\Theta_D^Q = 98(6)$ K and $\Theta_D^S = 90(10)$ K respectively.

1. Introduction

Since the first discovery of solid highly pressurized inert gas precipitates at room temperature in metals in 1984 [1, 2], numerous studies have been carried out using a range of metal–inert-gas systems [3–15]. Solid FCC and HCP inert gas precipitates of Ar, Kr and Xe have been observed to be epitaxial with a variety of metallic host matrices. Interesting phenomena such as bubble lattice formation were reported. From a fundamental point of view the solid inert gas precipitate provides a convenient object for the study of the behaviour of small assemblies of particles, a model system for precipitation under ion bombardment and a useful miniature high-pressure laboratory.

Mössbauer spectroscopy on the 9.4 keV transition in ^{83}Kr is a very interesting method for the study of these highly compressed precipitates. Different environments of the Kr atom give rise to clearly different components in the spectrum. In particular, the contribution of bulk and interface bubble atoms can be separated. From the relative intensities the size of the bubble can be inferred. The lattice dynamics can be studied directly by monitoring the recoilless fraction as a function of temperature, from which the characteristic Mössbauer temperature can be derived. This quantity and the isomer shift are directly related to the atomic density in the bubbles.

Notwithstanding the favourable characteristics of the Mössbauer transition in ^{83}Kr, the methodology of this resonance is not very well developed. This is due to the fact that solid state Kr systems are a rare phenomenon. The most suitable parent isotope is ^{83}Rb (86 d), but the preparation of a single-line ^{83}Rb source turns out to be a difficult problem.

Measurements with an ^{83}RbCl source on an ^{83}KrAl absorber have already been published [16, 17]. The spectra were fitted with two components: a single line (associated with

0953-8984/93/223541+14$07.50

atoms in the bulk of the solid precipitates) and a component split by quadrupole interaction (associated with atoms at the Kr–Al interface). It was assumed that the electrical field gradient V_{zz} is axially symmetric. Consequently the $7/2^+$ to $9/2^+$ transition in the Mössbauer nucleus gives rise to 11 lines in the quadrupole split component. The quadrupole moment Q for the ground state is +0.0260(7) barn [18] while the ratio of quadrupole moments for excited and ground states is given by $Q_i/Q_f = 1.958(2)$ [19]. Thus three position parameters where necessary to fit the whole spectrum, the isomer shifts of both components and the quadrupole coupling $\Delta = eQV_{zz}$. The result for the single line was $S = +0.029(5)$ mm s^{-1}, while for the other component $S = +0.017(7)$ mm s^{-1} and $\Delta = +1.83(6)$ mm s^{-1}. There was no indication for the presence of a single line with $S = +0.68(3)$ mm s^{-1} that was ascribed earlier to substitutional ^{83}Rb atoms in Al [20].

Spectra obtained at 4.2 K after vacuum annealing for 20 min at various temperatures showed a gradual increase of the intensity of the single line, associated with bubble growth. However, even after annealing at 700 K the quadrupole component still had a relative intensity of 56%. The original analysis of the data implicitly assumed that the ^{83}RbCl source gives rise to a single line, as expected for a cubic environment. However, later experiments have shown that this is not the case [17]. To demonstrate this, several spectra are compared in figure 1. Figure 1(*a*) shows the spectrum taken on ^{83}RbCl versus solid Kr, while (*b*) shows the spectrum taken on ^{83}RbCl versus the ^{83}KrAl absorber which was annealed at 750 K for 2 h. Since there is hardly any difference between the two spectra, this strongly suggests that the observed quadrupole splitting is not caused by the absorbers, but originates from the source. This implies that after annealing to 700 K the Kr bubbles have grown to such a size that the fraction of interface atoms is negligible with respect to the bulk fraction.

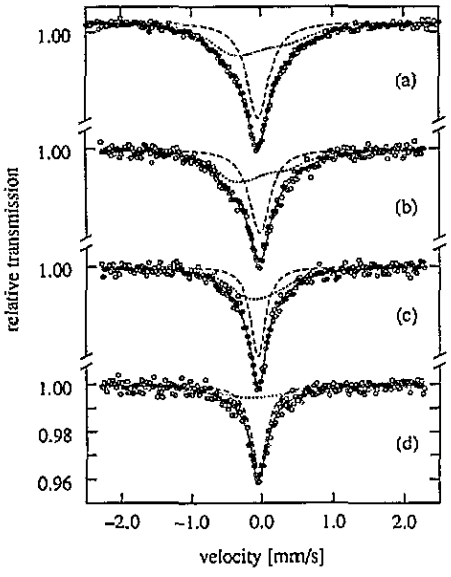

Figure 1. Spectra taken at 4.2 K of (*a*) ^{83}RbCl versus solid Kr, (*b*) ^{83}RbCl versus ^{83}KrAl annealed at 750 K for 2 h, (*c*) ^{83}RbI versus solid Kr and (*d*) dehydrated ^{83}RbI versus solid Kr.

In order to obtain a single-line source we made $^{83}RbHF_2$, ^{83}RbCl and ^{83}RbI sources, which were measured versus solid Kr and the ^{83}KrAl absorber. Whereas the spectra taken

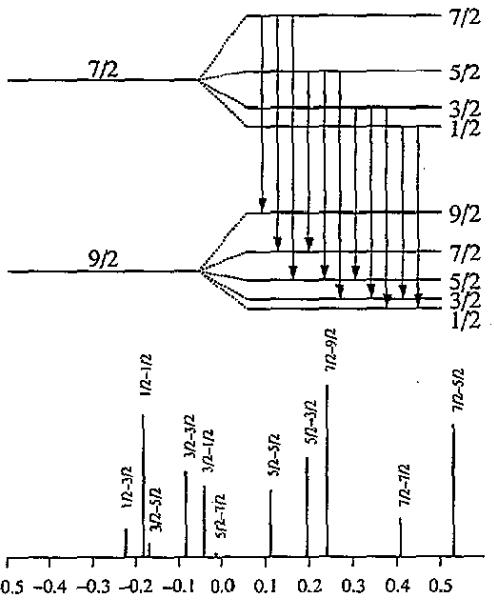

Figure 2. Diagram of the $7/2^+$ to $9/2^+$ transition in ^{83}Kr. The top part shows the splittings of the ground and excited states due to an electrical field gradient V_{zz} and the 11 transitions. The bottom part shows the relative intensities of these transitions and their energies with respect to an unsplit transition, in units of eQV_{zz}.

with the $^{83}RbHF_2$ source show very broad lines, the ^{83}RbI spectra are narrower than those of ^{83}RbCl (figure 1(*c*)). As a next step we dehydrated the ^{83}RbI source at 100 °C for half an hour under H_2 flow, which narrows the line even more and decreases the intensity of the quadrupole split component (figure 1(*d*)). Apart from the distortion of cubic symmetry by hydration, electronic after-effects in the decay from ^{83}Rb to ^{83}Kr may also be partially responsible for the quadrupole component. After-effects will be smaller in RbI than in RbCl because the former compound is more covalent.

Instead of reanalysing the original data, we decided to perform new measurements on a similar KrAl sample using an ^{83}RbI source. The analysis of the measurements must take into account the quadrupole split behaviour of the source together with the quadrupole split behaviour of the absorber. The total spectrum then consists of four contributions: the source single line convoluted with the absorber single line (ss), the source quadrupole component convoluted with the absorber single line (qs), the source single line convoluted with the absorber quadrupole component (sq) and the source quadrupole component convoluted with the absorber quadrupole component (qq). In the following we will derive expressions of these four contributions.

2. Mössbauer spectra for quadrupole split source and absorber

If a Mössbauer nucleus is in a site with a point group symmetry less than cubic, the nucleus will experience an electrical field gradient with largest component $V_{zz} = \partial^2 V/\partial z^2$. The interaction with the nuclear quadrupole moment Q gives rise to an electrical quadrupole interaction which, within the nuclear manifold with spin I, can be expressed as

$$H_Q = eQV_{zz}[3I_z^2 - I(I+1) + \eta(I_x^2 - I_y^2)]/4I(2I-I) \qquad (1)$$

with η, the asymmetry parameter, defined as

$$\eta = (V_{xx} - V_{yy})/V_{zz}. \tag{2}$$

This interaction leads to a splitting of the nuclear levels. If the site has a threefold or higher axis of symmetry, the asymmetry parameter is zero. In this case the energy levels are given by

$$E_m = eQV_{zz}[3m^2 - I(I+1)]/4I(2I-I) \tag{3}$$

where $m = -I, \ldots, +I$. The transition energies between excited and ground state are given by

$$\Delta E = E_{m_i} - E_{m_f} = eQV_{zz}\{[-3m_f^2 + I_f(I_f+1)]/4I_f(2I_f-1) + R_Q[3m_i^2 - I_i(I_i+1)]/4I_i(2I_i-1)\} \tag{4}$$

where $R_Q = Q_i/Q_f$ and i and f refer to initial and final states respectively (figure 2). The Mössbauer transition of ^{83}Kr has a magnetic dipole (M1) character with a small electric quadrupole (E2) admixture [21]. Making the approximation of pure 2^l-pole radiation, the intensity I of the emitted radiation between $|I_i, m_i\rangle$ and $|I_f, m_f\rangle$ is proportional to the following [22]

$$I\alpha \begin{pmatrix} I_f & l & I_i \\ m_f & m & -m_i \end{pmatrix}^2 \tau_m^l(\beta). \tag{5}$$

The absorption probability Σ between the absorber eigenstates $|I_i', m_i'\rangle$ and $|I_f', m_f'\rangle$ is proportional to the following:

$$\Sigma\alpha \begin{pmatrix} I_f' & l' & I_i' \\ m_f' & m' & m_i' \end{pmatrix}^2 \tau_{m'}^{l'}\beta \cos^2\theta \equiv I' \cos^2\theta \tag{6}$$

where $I_i' \equiv I_f$ and $I_f' \equiv I_i$. In the absence of any preferential orientation in source and absorber, the Mössbauer pattern for thin absorbers is given by

$$\int\int\int I\Sigma = \int\int\int II' \cos^2\theta \, \mathrm{d}\phi \, \mathrm{d}\beta \, \mathrm{d}\beta' \tag{7}$$

where $\cos^2\theta$ and τ are functions of the transitions m and m' and the Euler angles α, α', β and $\beta'(\phi = \alpha - \alpha')$ in source and absorber respectively (figure 3). The integral can be evaluated analytically and equation (7) reduces to

$$\int\int\int I\Sigma = II' \begin{cases} \frac{1}{4}\pi^3 & m=0 \quad m'=0 \\ \frac{3}{4}\pi^3 & m=0 \quad m'=1 \\ \frac{1}{2}\pi^2(1+\frac{1}{8}\pi) & m=1 \quad m'=1. \end{cases} \tag{8}$$

So the quadrupole–quadrupole convolution consists of 121 Lorentzian lines, where the relative intensities are given by (8) and the transition energies by

$$\Delta E = \Delta E_s - \Delta E_a. \tag{9}$$

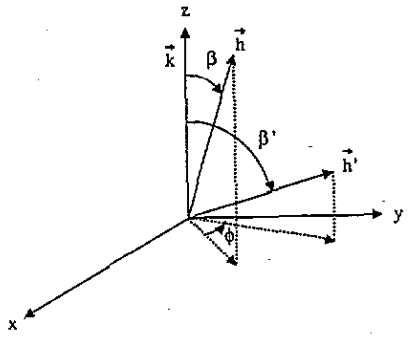

Figure 3. Euler angles α, $\alpha'(\phi = \alpha - \alpha')$ and β, β' of the quantization axes h, h' for the source (unprimed) and absorber (primed). k is the direction of propagation of the γ ray.

The transition energies ΔE in source and absorber are defined in equation (4).

To fit a Mössbauer spectra where both source and absorber consist of a single line and an axial quadrupole component, 15 parameters are necessary:

background	B				(i)
single line–single line	A_{ss}	S_{ss}		Γ_{ss}	(ii–iv)
quadrupole–single line	A_{qs}	S_{qs}	Δ_{qs}	Γ_{qs}	(v–viii)
single line–quadrupole	A_{sq}	S_{sq}	Δ_{sq}	Γ_{sq}	(ix–xii)
quadrupole–quadrupole	A_{qq}	S_{qq}	$(\Delta_{qs}\Delta_{sq})$	Γ_{qq}	(xiii–xv)

where B, A, S, Δ and Γ represent background, area, isomer shift, quadrupole coupling and linewidth respectively and the subscripts s and q stand for single line and quadrupole, where the first position refers to the source and the second to the absorber. By measuring the quadrupole split source versus a single-line absorber X the quadrupole split nature of the source can be eliminated from the model. From such a measurement the following parameters can be obtained:

$$c_1 \equiv (S_{qs} - S_{ss})_X \qquad c_2 \equiv (A_{qs}/A_{ss})_X$$
$$c_3 \equiv (\Delta_{qs})_X \qquad c_4 \equiv (\Gamma_{qs} - \Gamma_{ss})_X$$

which gives

$$A_{qs} = A_{ss}c_2 \qquad S_{qs} = S_{ss} + c_1 \qquad \Delta_{qs} = c_3 \qquad \Gamma_{qs} = \Gamma_{ss} + c_4$$
$$A_{qq} = A_{sq}c_2 \qquad S_{qq} = S_{sq} + c_1 \qquad \Gamma_{qq} = \Gamma_{sq} + c_4.$$

So the 15-parameter model can be reduced to an eight-parameter model, similar to the case of a single-line source: B, A_{ss}, S_{ss}, Γ_{ss}, A_{sq}, S_{sq}, Δ_{sq} and Γ_{sq} labelled a_1 to a_8.

If we also allow for a second-order Doppler shift in the single-line and quadrupole split components, $S_3(T)$ and $S_6(T)$ respectively, then the fitting function F is defined as follows:

$$F(v, T) = a_1 \left\{1 - (2/\pi)[F_{ss}(v, T) + F_{qs}(v, T) + F_{sq}(v, T) + F_{qq}(v, T)]\right\} \tag{10a}$$

$$F_{ss}(v, T) = (a_2/a_4)\left\{[a_3 + S_3(T) - v]^2 + (a_4/2)^2\right\}^{-1} \tag{10b}$$

$$F_{qs}(v, T) = c_2 \frac{a_2}{a_4 + c_4} \sum_{i=1}^{11} \frac{I_i}{(a_3 + S_3(T) + c_1 - c_3E_i - v)^2 + [(a_4 + c_4)/2]^2} \tag{10c}$$

$$F_{sq}(v,T) = \frac{a_5}{a_8}\sum_{i=1}^{11}\frac{I_i}{(a_6 + S_6(T) + a_7E_i - v)^2 + (a_8/2)^2} \tag{10d}$$

$$F_{qq}(v,T) = c_2\frac{a_5}{a_8 + c_4}\sum_{ij=1}^{11}\frac{I_{ij}}{(a_6 + S_6(T) + c_1 - c_3E_i + a_7E_j - v)^2 + [(a_8 + c_4)/2]^2} \tag{10e}$$

where the isomer shifts a_3 and a_6 are defined as $S_{ss}(0\text{ K})$ and $S_{sq}(0\text{ K})$ respectively, and the transition energies E_i are defined as ΔE in equation (4).

In order to fit the measured spectra a dedicated computer program was written. The program is able to fit a series of measured spectra to the described model by the fitting algorithm of Marquardt [24]. Several parameters can be optimized simultaneously, where optimization of a parameter means finding the value of the parameter, taken to be the same in all spectra, for which the whole set of spectra has the lowest χ^2. Second-order Doppler shifts are included as predicted by the Debye model.

3. Experimental results

^{83}Kr was implanted at room temperature in Al foils of 1.3 μm thickness at an energy of 110 keV to a total dose of 1.7×10^{16} Kr cm^{-2}, corresponding to a maximum atomic concentration of ~ 4 at.%. Transmission electron microscopy (TEM) experiments show that under these conditions small solid precipitates are formed, which are epitaxial with the Al matrix [5,6,23]. For the Mössbauer experiments a total area of 70 cm^2 was implanted at both sides, from which an absorber of 1.5×10^{18} cm^{-2} was made, corresponding to a Mössbauer thickness of $t = 1.5$ at 4.2 K.

Table 1. *Source parameters, in mm s^{-1}.*

Source	A_{qs}/A_{ss}	S_{qs}	S_{ss}	Δ_{qs}	Γ_{qs}	Γ_{ss}
Dry	0.44(5)	−0.04(2)	−0.040(3)	2.1(4)	0.71(9)	0.30(2)
Humid	0.6(1)	—	—	1.9(6)	—	—
Wet	1.32(5)	—	—	−1.3(9)	—	—

As a source we used 0.5 mCi of ^{83}RbI, produced via the ^{85}Rb(p,3n)^{83}Sr reaction. A target of 750 mg cm^{-2} natural RbCl was irradiated with 45 MeV protons to a total dose of 60 μA h, using the KVI cyclotron in Groningen. The resulting ^{83}Sr activity was chemically separated and allowed to decay to ^{83}Rb (86 d), after which a thin ^{83}RbI source was made. Mössbauer spectroscopy was performed in transmission geometry, using an Si(Li) detector. During the measurement the source was always kept at 4.2 K, while the absorber temperature could be varied from 4.2 K to 230 K. In addition measurements were performed at 4.2 K on a 2.4 mg cm^{-2} solid Kr layer absorbed on the outer side of the Be window of the liquid He cryostat.

In order to determine the quadrupole solid nature of the source, we measured the ^{83}RbI source versus the ^{83}KrAl absorber which was annealed at 750 K for 2 h. The Mössbauer experiments were done with three ^{83}RbI sources. During the course of the experiments it became clear that a dry ^{83}RbI source is hydrated within a minute in air at room temperature. The best result was obtained by assembling the source in a dry box and quickly cooling to

80 K. Unfortunately this was not done for all ^{83}RbI sources, which consequently differ in water content. They are called the dry, humid and wet source, respectively.

The measurement spectra are shown in figure 4, while the results are summarized in table 1. It turns out that we can obtain satisfactory fits by keeping the linewidths and isomer shifts the same in all three measurements. We see that the ratio of the area of the quadrupole split component to the area of the single-line component of the ^{83}RbI source shows an increase, while the quadrupole coupling constant shows a decrease and sign reversal upon an increased hydration of the source. This effect must be due to a distortion of the cubic symmetry around the ^{83}Rb ions in the rock salt structure of the source, caused by the introduction of water molecules. We will not comment on these values but only use them to obtain the parameters c_1–c_4. These are listed in table 2.

Table 2. Source specification.

Source	c_1	c_2	c_3	c_4
Dry	0.00(2)	0.44(5)	2.1(4)	0.41(9)
Humid	—	0.6(1)	1.9(6)	—
Wet	—	1.32(5)	−1.3(9)	—

Table 3. Optimized absorber parameters, in mm s^{-1}.

	S_s	Δ_s	Γ_s
S	0.064(2)	—	0.511(8)
Q	0.106(2)	1.33(9)	0.591(6)

Table 4. Total absorbed area of both components.

Source	T(K)	A_{tot}	A_{ss}	A_{sq}
Dry (○)	4.2	0.003 40(2)	0.001 35(1)	0.002 05(2)
	20	0.003 33(4)	0.001 21(2)	0.002 12(3)
	40	0.002 94(4)	0.001 05(2)	0.001 89(3)
	60	0.003 06(4)	0.000 83(2)	0.002 23(3)
Humid (+)	4	0.003 14(4)	0.000 79(2)	0.002 35(3)
	100	0.002 32(2)	0.000 65(1)	0.001 67(2)
	150	0.001 87(2)	0.000 55(1)	0.001 32(2)
	200	0.001 59(2)	0.000 36(1)	0.001 23(2)
Wet (×)	4	0.003 77(2)	0.000 959(8)	0.002 81(2)
	80	0.003 04(1)	0.000 750(6)	0.002 29(1)
	150	0.001 98(2)	0.000 460(9)	0.001 52(2)

With these three sources we performed a series of Mössbauer experiments versus the as-implanted ^{83}KrAl absorber at different temperatures from 4 to 200 K (figures 5–7). When fitting these spectra with the function defined in equation (10α) we kept the line widths and the quadrupole coupling constant the same for all spectra, while the isomer shifts of both components were allowed to vary according to the second-order Doppler shift. The resulting values for these five parameters are given in table 3 (S_{ss} and S_{sq} are the values of the isomer shifts at 0 K).

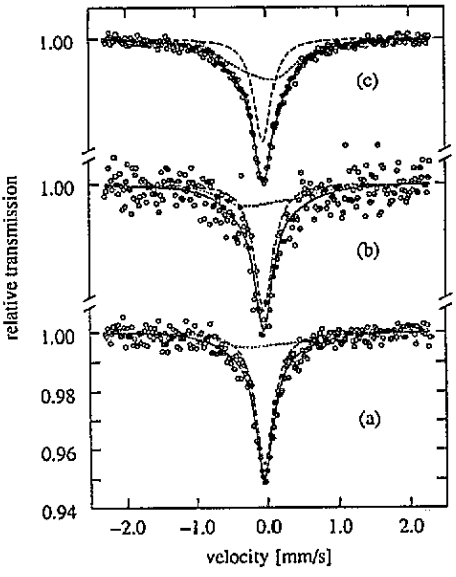

Figure 4. Spectra taken at 4.2 K of (*a*) dry, (*b*) humid and (*c*) wet ^{83}RbI source versus the ^{83}KrAl absorber annealed at 750 K for 2 h.

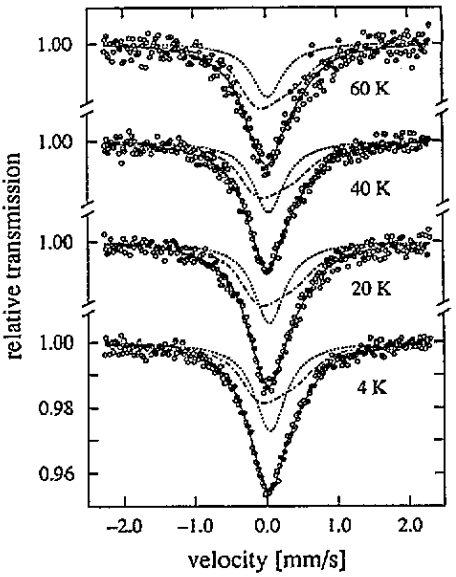

Figure 5. Spectra taken at the indicated temperatures with the dry ^{83}RbI source versus the as-implanted ^{83}KrAl absorber.

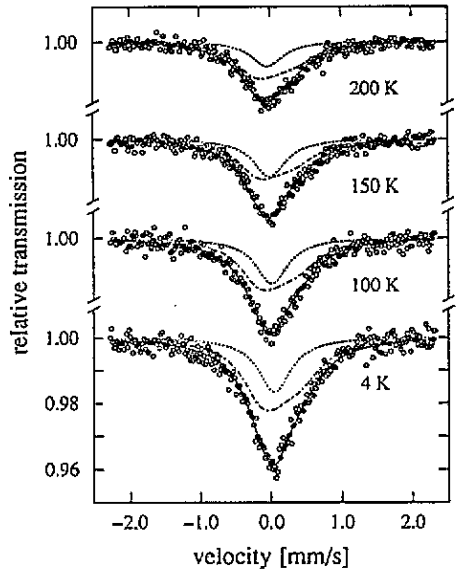

Figure 6. Spectra taken at the indicated temperatures with the humid ^{83}RbI source versus the as-implanted ^{83}KrAl absorber.

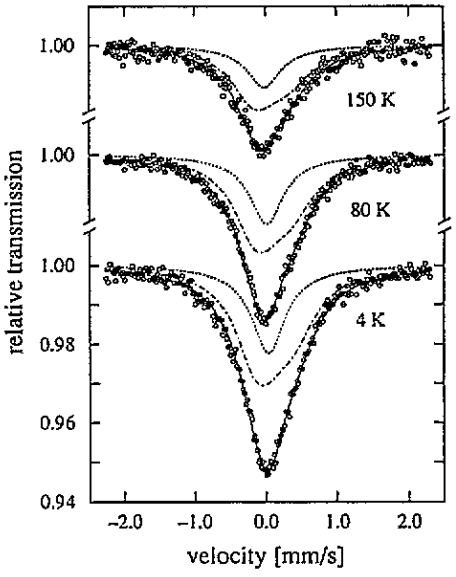

Figure 7. Spectra taken at the indicated temperatures with the wet ^{83}RbI source versus the as-implanted ^{83}KrAl absorber.

The areas of $A_{ss} + A_{sq} \equiv A_{tot}$, A_{ss} and A_{sq} for the three sources as a function of temperature are listed in table 4. There exist variations of less than 10% in the overall

areas of several runs. This is due to different peak-to-background ratios in the window on the 9.4 keV Mössbauer line. If we assume a simple Debye model, the total absorbed area A_{tot} can be fitted to obtain the characteristic Debye temperature Θ_D^T. The areas as a function of temperature normalized to 1 are plotted in figure 8(*a*). The fit to a Debye model yields $\Theta_D^T = 101(2)$ K. As can be seen, although the data points show some scatter around the fit to the Debye model, the results of the measurements with three different sources yield a consistent picture. Another important check is the relative area of the single-line component (at 4.2 K) which should be independent of the shape of the source. This relative area turned out to be 39.6(6)%, 25.4(3)% and 25.2(7)% for the dry, humid and wet sources respectively, where the errors do not take into account the uncertainty in the source parameters. The areas of single line A_{ss} and quadrupole component A_{sq} as a function of temperature normalized to 1 are plotted in figures 8(*b*) and (*c*). As can be seen from the figure, the temperature dependence of the absorbed areas taken with the dry source show a somewhat different behaviour than for the humid and wet sources. Nevertheless the temperature dependence of A_{sq} can be fitted quite well with a Debye model yielding a Debye temperature for the quadrupole component $\Theta_D^Q = 98(6)$ K. The large scatter of the data points for the temperature dependence of A_{ss} makes it very difficult to derive a Debye temperature of the single-line component. However, there is indication that Θ_D^S for the bulk ^{83}Kr is somewhat lower than for the interface atoms. An individual Debye fit of the areas of the single line for dry, humid and wet sources yields $\Theta_D^S = 62(1)$, 98(7) and 88(6) K respectively, yielding an average Debye temperature of $\Theta_D^S = 83(6)$ K. However, an overall fit yields $\Theta_D^S = 95(5)$ K. We estimate $\Theta_D^S = 90(10)$ K.

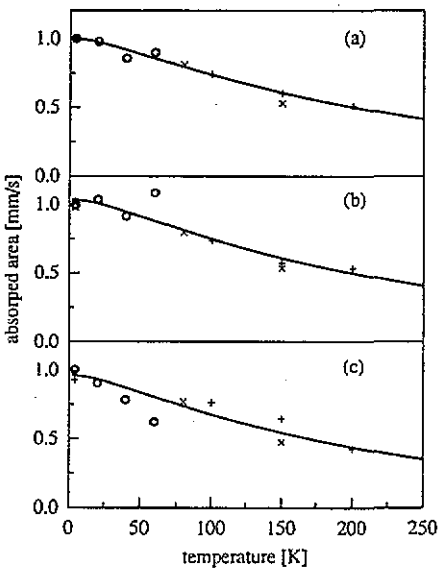

Figure 8. Absorbed area of the spectra taken with dry (○), humid (+) and wet (×) ^{83}RbI source, figures 5, 6 and 7 respectively, versus as-implanted ^{83}KrAl as a function of absorber temperature. Plotted are the normalized areas of table 4 of the total spectrum (*a*), quadrupole component (*b*) and single line (*c*). The data are fitted to a Debye model and yield $\Theta_D^T = 101(2)$ K, $\Theta_D^Q = 98(6)$ K and $\Theta_D^S = 90(10)$ K respectively.

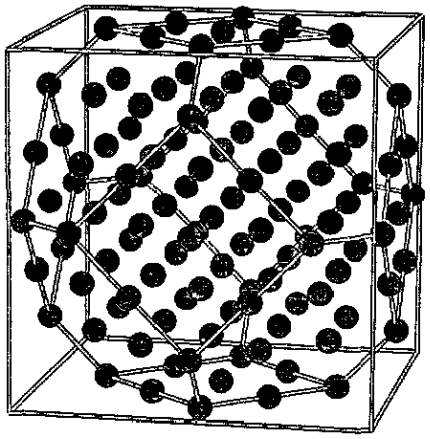

Figure 9. Schematic drawing of a cuboctahedral FCC precipitate. The precipitate is bounded by eight{111} and six {100} planes. Shown is a cuboctahedron with six {111} planes, cut off after two {111} planes by a {100} plane. The total number of atoms is 116, the bulk fraction is 33%.

4. Discussion

A simple interpretation of the two components in the analysis of the KrAl absorber already put forward in the previous publications on this system [16, 17] would be that the single line is due to atoms in the bulk of the precipitates, while the quadrupole component is associated with atoms on the Kr–Al interface. Various experiments on the depth dependence of the quadrupole interaction have shown that a large surface electrical field gradient (EFG) is present only for the outermost layer, with atoms in the second layer experiencing an EFG of at most 15% of the surface EFG [27, 28, 30]. From the measured quadrupole coupling constant, we derive an interface EFG, $V_{zz} = +1.7 \times 10^{17}$ V cm^{-2}, which is 30% lower than in the original analysis. The sign is in agreement with that for a metal–vacuum interface [26–28]. The value for V_{zz} should be interpreted as an average over various interface sites. TEM experiments on Xe precipitates in Al [9] show that the precipitate is bounded predominantly by {111} planes, with contributions also by {100} planes. In addition, there will be various edge sites. These will give rise to different quadrupole split components in the Mössbauer spectrum. Because the spectra do not have sufficient resolution to observe these sites directly, their existence is consistent with the relatively large line width Γ_{sq} of the quadrupole split component.

The size of the precipitates can be determined from the relative fraction of the single-line component. Because of the relatively large errors in the determination of the source parameters of the humid and wet sources, we estimate a relative fraction of 30–35%. Among others, studies on Xe precipitates in Al [9] as well as on inert gases in Cu [25] suggest that the Kr precipitates have a cuboctahedral shape, i.e. bounded predominantly by eight {111} planes and six smaller {100} planes (figure 9). If we assume a cuboctahedral shape, the bulk fraction for six planes in the {111} direction is 30%, and for seven planes 37%. The size of an octahedral precipitate can be defined as the distance L between two parallel interfacial {111} planes, given by $L = aN/\sqrt{3}$, where a is the lattice constant and N the

number of {111} planes. TEM shows that the high-dose implantations of Kr in Al at room temperature lead to the formation of small solid precipitates epitaxially aligned with the Al matrix [5, 6, 23]. The molar volume derived from the extra Kr reflections is 22.8 cm^3, corresponding to a lattice parameter of $a = 5.330$ Å. Thus, the relative fraction of the single line of 30–35% yields a precipitate size of 15–18 Å. This is in good agreement with the original result and TEM estimates. For a cuboctahedron the size of the precipitates will be somewhat smaller.

The width of the substitutional line $\Gamma_{ss} = 0.511(8)$ mm s^{-1} is 70% larger than found for large Kr precipitates or solid Kr layer (table 1: 0.30(2) mm s^{-1}). The strain distribution in the bubbles may cause some line broadening, but it is improbable that this can explain the whole effect. However, the second-layer atoms and maybe also part of the interface may have a relatively small quadrupole interaction, such that their contribution is contained in the broadened single line. Unfortunately, the shape of the spectra does not permit an unambiguous fit with a single-line and two quadrupole components. We have to conclude that our two-component model is probably too simple to describe the physical situation precisely. Hence, we have to be careful with the interpretation of the parameters derived.

In the original analysis with an ^{83}RbCl source the isomer shift of the single line at 4.2 K shows a gradual decrease from +0.029(5) mm s^{-1} on the as-implanted sample to −0.021(4) mm s^{-1} on the sample annealed at 700 K. The decrease is towards the isomer shift of solid Kr, −0.032(2) mm s^{-1} as measured with an ^{83}RbCl source. In the present analysis with the ^{83}RbI sources, the as-implanted sample has an isomer shift of +0.064(2) mm s^{-1}, while the isomer shift of the sample annealed at 700 K yields −0.040(3) mm s^{-1}, which is equal to the isomer shift of solid Kr as measured with ^{83}RbI, −0.041(2) mm s^{-1}. The result of the present analysis is more reliable because the quadrupole split nature of the source is taken into account. The gradual decrease of 0.104(3) mm s^{-1} upon annealing reflects the fact that the s density decreases under decompression. The isomer shifts of ^{83}RbCl and ^{83}RbI versus solid Kr are +0.032(2) mm s^{-1} and +0.040(3) mm s^{-1} respectively. This means that the s density at the ^{83}Rb nucleus is greater in the latter salt. Probably the more covalent nature of the Rb–I bonding leads to a somewhat larger number of p holes in the Kr $4s^2p^6$ shell. The number of p holes h_p can be estimated on the basis of a result of Holloway *et al* [19] obtained by Mössbauer spectroscopy on KrF_2 and $KrF_2{\cdot}MF_5$ (M = As,Sb) absorbers, using an ^{83}RbF source. They found a relation between the observed isomer shift and the number of p holes: $S \simeq 1.45\ h_p$. Using this relation, we derive $h_p \simeq 0.046(3)$ and 0.058(4) respectively. The isomer shifts of the various sources versus solid Kr (4.2 K) of the as-implanted KrAl sample and the sample annealed at 700 K are summarized in table 5.

Table 5. Isomer shifts versus solid Kr (4.2 K) in mm s^{-1}.

	$^{83}RbHF_3$	^{83}RbCl	^{83}RbI	^{83}KrAl (as-implanted)	^{83}KrAl (annealed at 700 K)
S	+0.03(2)	+0.032(2)	+0.041(2)	+0.105(3)	+0.001(3)
Δ	—	—	—	+0.13(3)	−0.03(3)

Although it turned out to be difficult to derive an accurate value for the characteristic Debye temperatures of single-line and quadrupole components, as was discussed in a previous section, there is an indication that Θ_D^S is somewhat lower than Θ_D^Q, i.e. 90(10) and 98(6) K. A somewhat larger characteristic temperature of the interface atoms is consistent with the fact that the Al lattice is much stiffer than the Kr solid. Similar results have been obtained from Mössbauer data on ^{133}Xe in W [29], where the interface characteristic

temperature is about 20% larger than the bulk characteristic temperature. However, the characteristic temperature of the single-line component is also appreciably larger than the value for solid Kr at atmospheric pressure. This reflects the fact that the molar volume in the small precipitates is much smaller than for solid Kr at ambient pressure, leading to higher phonon frequencies. The molar volume is practically constant during our temperature dependent measurements, because the total volume of the precipitate is determined by the Al matrix. Consequently, the phonon spectrum does not change as a function of temperature, which implies that the effective Debye temperature is temperature independent. Indeed, the Debye model yields a good fit to the data over the whole temperature range, in contrast to the situation for solid Kr at ambient pressure [21].

In the Debye model of a solid, the volume dependence of the Debye temperature, defined as the Grüneisen parameter γ, in general a function of temperature and volume, is given by

$$\gamma = -\partial \ln \Theta_D / \partial \ln V \tag{11}$$

or

$$(\partial \Theta_D / \partial V)_T = -\gamma \Theta_D / V. \tag{12}$$

Fugate and Swenson [31] have used a reduced equation of state (EOS) for Ne which follows from direct C_v data and a volume dependence of Θ_0 (effectively γ) to derive a C_p (T, $p = 0$) relation which agrees well with direct measurements. This EOS is also consistent with a measurement by Anderson *et al* [32] if it is assumed that

$$\gamma = \text{constant} \times V. \tag{13}$$

Holt and Ross [33] found the same linear relation. They calculated the volume dependent values for the Grüneisen parameter for Ar and Xe for five different models, all of which used a similar form for the interatomic potential.

If γ / V is constant ($= \gamma_0 / V_0$), equation (12) has the solution

$$\Theta_D = \Theta_{D_0} \exp[\gamma_0 (1 - V/V_0)] \tag{14}$$

where the subscript 0 refers to the values at some reference temperature and pressure. If we choose the melting point of Kr at 1 bar for this reference ($T_m = 116.5$ K), we have $\Theta_{D_0} = 51.6(5)$ K [16, 34], $V_0 = 29.88$ cm^3 mol^{-1} [36] and $\gamma_0 = 2.27$ [35].

For the as-implanted precipitates we have $V = 22.8$ cm^3 mol^{-1}, as determined by TEM experiments on similar samples [5, 6, 23]. Using equation (14) we derive $\Theta_D = 88(1)$ K, which compares well with the direct measurement of Θ_D^S for the single-line component, $\Theta_D^S = 90(10)$ K. We can also apply equation (14) to solid Kr at 1 bar and 0 K, where $V = 27.10$ cm^3 mol^{-1} [36]. This yields $\Theta_D = 64(1)$ K, in perfect agreement with the value measured at low T on large Kr precipitates in Al: 63.7(1.0) K [16]. We conclude that equation (14), derived for bulk material, gives also an adequate description of the volume dependence of the phonon spectrum in the small precipitates.

5. Conclusion

Mössbauer spectroscopy on ^{83}Kr is hampered by the fact that no good single-line source is available at the moment. However, we have shown that the analytical deconvolution

technique presented here enables us to fit the data for ^{83}KrAl in a consistent way, using a two-component model. Assuming that the quadrupole components results from Kr atoms at the interface, we find that the size of the precipitates is 1.5–1.8 nm, in good agreement with TEM. The analysis shows that interface atoms have a somewhat higher Debye temperature than atoms in the bulk of the precipitate. The values for Θ_D can be understood on the basis of the volume dependence of the phonon spectrum. The isomer shift of the bulk fraction is significantly larger than of a solid Kr layer, reflecting the fact that the s density increases under compression.

Acknowledgments

The authors wish to thank F Th ten Broek for his help in preparing the radioactive sources, J J Smit for operating the mass separator and L Venema for preparing the Al foils. We appreciate the help of the staff of the KVI cyclotron during the production of the ^{83}Sr activity. We acknowledge useful discussions with A van Veen and H Pattyn. This work was performed as a part of the research programme of the Stichting voor Fundamenteel Onderzoek der Materie (FOM), with financial support from the Nederlandse Organisatie voor Wetenschappelijk Onderzoek (NWO).

References

[1] vom Felde A, Fink J, Müller-Heinzerling Th, Pflüger J, Schreerer B and Linker G 1984 *Phys. Rev. Lett.* **53** 922
[2] Templier C, Jaouen C, Rivière J-P, Delafond J and Grilhé J 1984 *C. R. Acad. Sci. (Paris)* **299** 613
[3] Tyagi A K, Khanna R and Rao G V N 1986 *Scr. Metall.* **20** 1245
[4] Cox R J, Goodhew P J and Evans J H 1987 *Acta Metall.* **35** 2497
[5] Birtcher R C and Jäger W 1986 *Nucl. Instrum. Methods* B **15** 435
[6] Birtcher R C and Jäger W 1987 *Ultramicroscopy* **22** 267
[7] Templier C, Garem H and Rivière J-P 1986 *Phil. Mag.* A **53** 667
[8] Templier C, Gaboriaud R J and Garem R 1985 *Mater. Sci. Eng.* **69** 63
[9] Donnelly S E and Rossouw C J 1985 *Science* **230** 1272
[10] Kuz'minov D B, Chernikov V N, Gerchikov M Yu, Panesh A M and Simonov A P 1989 *Sov. Tech. Phys. Lett.* **14** 846
[11] Khanna R, Tyagi A K, Nandedkar R V and Rao G V N 1986 *Scr. Metall.* **20** 181
[12] Evans J H and Mazey D J 1985 *J. Phys. F: Met. Phys.* **15** L1
[13] Evans J H and Mazey D J 1986 *J. Nucl. Mater.* **138** 176
[14] Templier C, Boubeker B, Garem H, Mathé E L and Desoyer J C 1985 *Phys. Status Solidi* a **92** 511
[15] Mitchell D R G and Donnelly S E 1990 *Radiat. Eff. Defects Solids* **114** 253
[16] Zhang G L and Niesen L 1989 *J. Phys.: Condens. Matter* **1** 1145
[17] Greuter M J W, Zhang G L, Niesen L, Buters F J M and van Veen A 1991 *Proc. Conf. on Fundamental Aspects of Inert Gases in Solids* ed S E Donnelly and J H Evans (New York: Plenum) p 231
[18] Stevens J G and Stevens V E 1978 *Mössbauer Data Index 1976* (New York: IFI Plenum) p 105
[19] Holloway J H, Schrobilgen G J, Bukshpan S, Hilbrants W and de Waard H 1977 *J. Chem. Phys.* **66** 2627
[20] Spijkervet W J J, Pleiter F and de Waard H 1980 *Hyperfine Interact.* **8** 173
[21] Kolk B 1974 *Thesis* Nuclear Solid State Physics, Groningen University
[22] Frauenfeld Ver H, Nagle D E, Taylor R D, Cochran D R F and Visscher W M 1962 *Phys. Rev.* **126** 1065
[23] Hashimoto I, Yorikawa H, Mitsuya H, Yamaguchi H, Takaishi K, Kikuchi T, Furuya K, Yagi E and Iwaki M 1987 *J. Nucl. Mater.* **149** 69
[24] Marquardt D W 1963 *J. Soc. Ind. Appl. Math.* **11** 431
[25] Schumacher R and Vianden R 1987 *Phys. Rev.* B **36** 8258
[26] Lindgren B 1987 *Hyperfine Interact.* **34** 217
[27] Korecki J and Gradmann U 1985 *Phys. Rev. Lett.* **55** 2491

[28] Korecki J and Gradmann U 1986 *Hyperfine Interact.* **28** 931
[29] Pattyn H, Hendrickx P and Bukshpan S 1991 *Proc. Conf. on Fundamental Aspects of Inert Gases in Solids* ed S E Donnelly and J H Evans (New York: Plenum) p 243
[30] Schatz G, Fink R, Klas T, Krausch G, Platzer R, Voigt J and Wesche R 1988 *Hyperfine Interact.* **49** 395
[31] Fugate R Q and Swenson C A 1973 *J. Low Temp. Phys.* **10** 317
[32] Anderson M S, Fugate R Q and Swenson C A 1973 *J. Low Temp. Phys.* **10** 345
[33] Holt A C and Ross M 1970 *Phys. Rev.* B **1** 2700
[34] Crawford R K 1977 *Rare Gas Solids* vol II, ed M L Klein and J A Venables (London: Academic) p 711
[35] Schlosser H and Ferrante J 1991 *Phys. Rev.* B **43** 13 305
[36] Korpiun P and Lüscher E 1977 *Rare Gas Solids* vol II, ed M L Klein and J A Venables (London: Academic) p 778